RESEARCH ARTICLE

Material Compound-Property Retrieval Using Electron Microscope Images for Rubber Material Development

RINTARO YANAGI[1], (Graduate Student Member, IEEE), REN TOGO[2], (Member, IEEE), KEISUKE MAEDA[2], (Member, IEEE), TAKAHIRO OGAWA[2], (Senior Member, IEEE), AND MIKI HASEYAMA[2], (Senior Member, IEEE)

[1]Graduate School of Information Science and Technology, Hokkaido University, Sapporo 060-0814, Japan
[2]Faculty of Information Science and Technology, Hokkaido University, Sapporo 060-0814, Japan

Corresponding author: Miki Haseyama (mhaseyama@lmd.ist.hokudai.ac.jp)

ABSTRACT This paper tackles the electron microscope image processing for rubber material discovery. In rubber material science fields, electron microscope images are used to observe the properties of materials during their development process. Hence, by analyzing the electron microscope images with the recent image processing technology, it is expected that further effective material developments can be realized. In this paper, we propose a rubber material compound and physical property image retrieval method using the rubber material electron microscope images. The aim of our method is to support material technologists to grasp the relationships between material compounds and physical properties visually and comprehensively. Our method constructs an electron microscope image space through a conditional image generation model. The generated images are used to retrieve materials with similar compounds and physical properties. By effectively using the constructed electron microscope image space, it is expected that the technologists visually and comprehensively understand the relationships of similar materials, and the advances in material developments are accelerated.

INDEX TERMS Electron microscope images, image retrieval, generative model, rubber materials.

I. INTRODUCTION

Rubber materials are one of the essential industrial materials in our daily life. They are used for various products, such as tires and sport items. Computer-aided analysis has been widely studied to accelerate the development of valuable rubber materials, and recent research has paid attention to the analysis with machine learning [1], [2], [3]. However, conventional studies mainly focus on the analysis of table and textual data obtained from materials [4], [5], [6], [7], and there are few studies focusing on electron microscope images of materials. By effectively analyzing the electron microscope images based on the recent image processing technologies, it is expected that rubber material developments can be accelerated.

General cycle of rubber material development is shown in Fig. 1. Rubber materials are first manufactured by mixing multiple base material compounds. Then, the manufactured rubber materials are evaluated to analyze their physical properties through demonstration experiments, such as driving tests. Finally, the evaluation results are used for reconsidering the properties of the base material compounds. By repeating this development cycle, material technologists obtain new knowledge about the materials and discover more valuable materials. The essential aim of the cycle is discovering more valuable materials; however, the conventional computer-aided analysis methods only focus on reducing the effort of the cycle and do not fully contribute to the
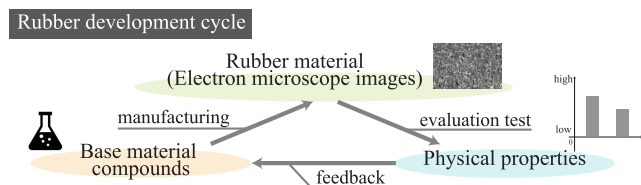
FIGURE 1. Rubber development cycle and images used in this paper. Our method supports material discovery using electron microscope images.
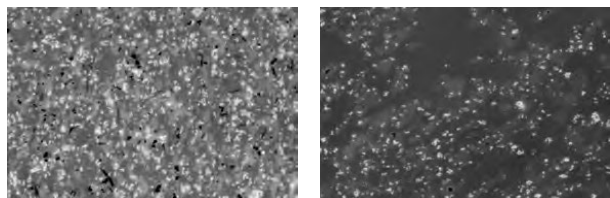

FIGURE 2. The electron microscope images used in our paper Each image is manufactured from different compound-property, respectively.

discovery [7], [8]. To effectively support the technologists, a method that mainly supports the discovery should be further considered.

To discover more valuable materials, it is essential to visually and comprehensively understand the relationships between rubber base material compounds and their physical properties (hereinafter referred to as compound-property) [9], [10], [11]. However, in conventional studies, comprehensively grasping the relationships is difficult since the inputs and outputs are associated in one-to-one correspondence. Furthermore, conventional studies mainly applied black-box machine learning models with complex parameter combinations, leading to lower explainability and unclear relationships for the technologists [4], [5], [6], [7]. In short, technologists cannot visually and comprehensively discover valuable rubber materials from conventional studies. If compound-property related to the technologist's interests can be visually and comprehensively observed, machine learning-based analysis that can further support material development is expected to be realized.

Among various machine learning-based methods, neural information retrieval is an effective way to comprehensively observe information, such as the compound-property [11], [12]. By ranking the compound-property related to the technologist's interests and plotting them adequately, it is considered that the technologists can comprehensively understand these relationships. However, the technologists cannot visually understand the inference reason since the general neural information retrieval methods handle high-dimensional features [13], [14], [15]. For the visual enumeration, the neural information retrieval should present the retrieval results with understandable information for the technologists. As such information, electron microscope images are useful. The electron microscope images can be obtained during the manufacturing process, and the technologists usually analyze

these electron microscope images to obtain new knowledge [16], [17], [18]. Figure 2 shows the electron microscope images used in this paper, and each image reflect the characteristics of input compound-property. By retrieving the compound-property using electron microscope images, machine learning-based analysis that can visually and comprehensively support the material discovery is expected to be realized.

In this paper, we propose a compound-property retrieval method using electron microscope images to support material discovery. Using electron microscope images, we can treat the compound-property retrieval as the image retrieval task. The proposed method retrieves compound-property highly related to the query compound-property. Here, to retrieve the related compound-property using the electron microscope images, it is required to prepare the electron microscope images corresponding to the query compound-property. However, manufacturing the corresponding electron microscope images every time takes much effort. To reduce such efforts, our method follows conditional image generation models [19], [20], [21], [22]. The proposed method generates an electron microscope image from the query compound-property using the conditional image generation model. Then by using the generated electron microscope image as a query, our method retrieves compound-property with similar electron microscope images. By enumerating the retrieved compound-property with these electron microscope images, visual and comprehensive machine learning-based analysis for rubber material developments is realized.

The contributions of this paper are summarized as follows.

Rubber material retrieval via images

To support the technologists, we propose the compound-property retrieval method using electron microscope images. Our method can support the technologists to visually and comprehensively discover new materials.

Image generation for rubber material

For visually providing the analysis results for the technologists, our method converts query compound-property into an electron microscope image. With its conditional image generation, our method enables visual and comprehensive retrieval without any further manufacturing effort.

II. RELATED WORKS
A. COMPUTER-AIDED RUBBER MATERIAL ANALYSIS
The computer-aided rubber material analysis methods mainly focus on assisting users to find new knowledge about rubber materials for manufacturing novel rubber materials. Specifically, these methods assist users by grasping the relationships between the base material compounds and the physical properties of the manufactured rubber material. Recently, for grasping these relationships, machine learning-based methods are frequently used for estimating one-to-one relationships between compound-property [4], [5], [6], [7]. Among
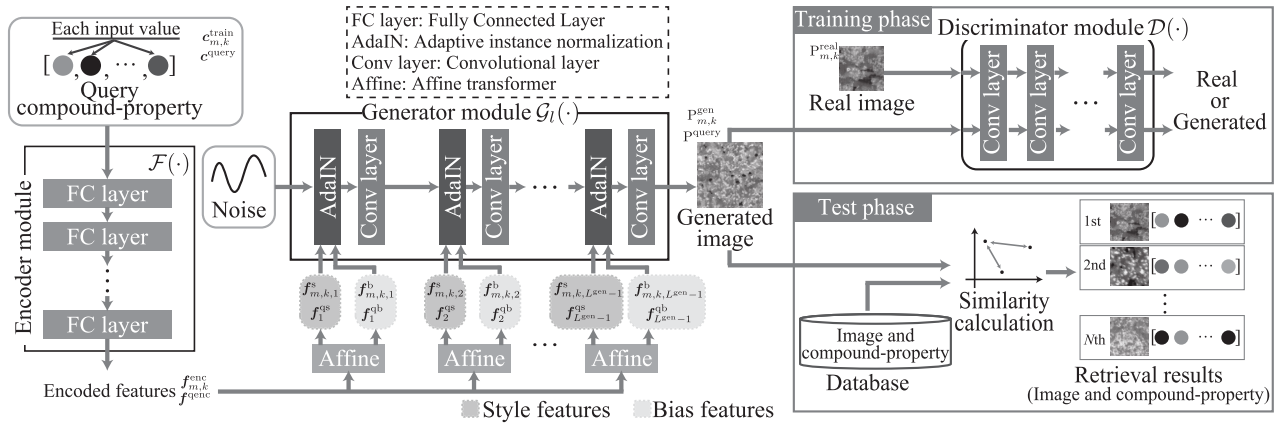
FIGURE 3. Overview of the proposed method. Our method first generates a microscope image from a query compound-property. Then, the generated and corresponding real images are passed into the discriminator module in the training phase. By training each module to generate images that the discriminator module mistakes for real images, our method is expected to generate realistic images corresponding to the query compound-property. In the test phase, the generated image is used to retrieve similar images in the database. By providing the retrieved images with the corresponding compound-property, visual and comprehensive machine learning-based support for the material discovery is expected to be realized.

them, the most relevant research is a method that estimates the physical properties from the electron microscope images of the rubber materials [8]. They can provide knowledge about one-to-one relationships between rubber material information by estimating the physical properties from the visual features extracted from the electron microscope images. Compared with them, our method can comprehensively provide analysis results with visual inference reasons by analyzing compound-property relationships via an image retrieval task. With its procedure, the computer-aided rubber material analysis that can further assist users in obtaining new knowledge is realized.

B. IMAGE GENERATION

With the recent progress of deep neural architectures, various image generation models such as variational autoencoders [23], generative adversarial networks (GAN) [24], and flow-based generative models [25] have been widely studied. Among these models, GAN has one of the most powerful generation abilities with its min-max game training strategies. The min-max game training is conducted with two modules of GAN: the generator module and the discriminator module. The generator module aims to generate realistic images that can deceive the discriminator module, and the discriminator module aims to discriminate real images and the images generated by the generator module.

Although the original GAN has powerful generation abilities, there were problems with the training stability and the limit of generated image resolution. To solve the training stability problem, WGAN [26] and WGAN-GP [27] introduce Wasserstein distance to the loss calculation. Compared with Jensen–Shannon divergence that is used in the original GAN, Wasserstein distance can suppress the vanishing gradient problem caused by non-overlapping between the probability distribution of real and generated data. To expand

the limit of generated image resolution, PGGAN [28] introduces a progressive growing strategy that gradually adds higher-resolution convolution and inverse convolution modules. With the gradually growing strategy, PGGAN can stably generate high-resolution images. Recently, by applying both Wasserstein distance and the progressive growing strategy, StyleGAN [21] can generate more realistic and high-resolution images. With its generation performance, we follow StyleGAN for generating rubber electron microscope images.

III. COMPOUND-PROPERTY RETRIEVAL USING ELECTRON MICROSCOPE IMAGES

This section presents the proposed compound-property retrieval method using electron microscope images. We show the overview of the proposed method in Fig. 3. The proposed method consists of the following two steps: conditional image generation and similar compound-property retrieval. First, we generate an electron microscope image P^{query} from a query compound-property $c^{query} \in \mathbb{R}^{D^c + D^p}$, where D^c and D^p represent the dimmensions of the compounds and physical properties, respectively. Then, the similarities s_n ($n = 1, 2, \ldots, N$; N is the number of candidate compound-properties) between the generated electron microscope image P^{query} and electron microscope images P_n^{cand} of candidate compound-property $c_n \in \mathbb{R}^{D^c + D^p}$ are calculated. Finally, the compound-property and electron microscope images highly related to the generated electron microscope image P^{query} are provided.

A. TRAINING OF CONDITIONAL IMAGE GENERATION MODEL

This subsection introduces the training procedure of our conditional image generation model $\mathcal{M}(\cdot)$. Our conditional image generation model is constructed based on

the conditional style generative adversarial network (Style-GAN) [21]. Since the electron microscope images have high resolution, we divide the training electron microscope images I_m^{train} ($m = 1, 2, \ldots, M$; M is the number of training electron microscope images) into M_m^{patch} patch images $P_{m,k}^{real}$ ($k = 1, 2, \ldots, M_m^{patch}$). Here, we define p_{real} as the probability distribution followed by $P_{m,k}^{real}$. Additionally, we represent the compound-property of each patch image $P_{m,k}^{real}$ as the vector $c_{m,k}^{train} \in \mathbb{R}^{D^c + D^p}$. Note that each dimension of $c_{m,k}^{train}$ is normalized based on the range of each compound-property.

Our conditional image generation model $\mathcal{M}(\cdot)$ consists of L^{enc}-layer encoder module $\mathcal{F}(\cdot)$, L^{gen}-layer generator module $\mathcal{G}_l(\cdot)$ ($l = 1, 2, \ldots, L^{gen}$), and L^{dis}-layer discriminator module $\mathcal{D}(\cdot)$. First, we extract representative features $f_{m,k}^{enc} \in \mathbb{R}^{D^{enc}}$ from the compound-property vector $c_{m,k}^{train}$ and random vector $z \sim N(\mu, \sigma^2) \in \mathbb{R}^{D^c + D^p}$ via the encoder module $\mathcal{F}(\cdot)$ as follows:

$$f_{m,k}^{enc} = \mathcal{F}(z, c_{m,k}^{train}), \tag{1}$$

where D^{enc} represents the dimension of the extracted encoder features; $f_{m,k}^{enc}$ represent features that should be reflected in the generated electron microscope image. By extracting the features $f_{m,k}^{enc}$ using the encoder module $\mathcal{F}(\cdot)$, compound-property vector $c_{m,k}^{train}$ is expected to be accurately reflected in the generated electron microscope images $P_{m,k}^{gen}$. Next, to apply the extracted features $f_{m,k}^{enc}$ to the generated images, we first translate the $f_{m,k}^{enc}$ into the style features $f_{m,k,l}^{s} \in \mathbb{R}^{D_l}$ and the bias features $f_{m,k,l}^{b} \in \mathbb{R}^{D_l}$ using the affine transformation $\mathcal{A}_l(\cdot)$, where D_l represents the dimension of the extracted l-th layer features. After that, we obtain the features $f_{m,k,l+1}^{in} \in \mathbb{R}^{D_l}$ for inputting $l + 1$-th layer generator module $\mathcal{G}_{l+1}(\cdot)$ by combining $f_{m,k,l}^{s}$ and $f_{m,k,l}^{b}$ into the output features $f_{m,k,l}^{out} \in \mathbb{R}^{D_l}$ of l-th layer generator module $\mathcal{G}_l(\cdot)$ as follows:

$$f_{m,k,l+1}^{in} = f_{m,k,l}^{s} \circ \frac{f_{m,k,l}^{out} - \mu(f_{m,k,l}^{out})}{\sigma(f_{m,k,l}^{out})} + f_{m,k,l}^{b}, \tag{2}$$

where $\circ$ represents Hadamard product. Equation (2) is an adaptive instance normalization-based transformation [29], and the features $f_{m,k}^{enc}$ extracted from the compound-property vector $c_{m,k}^{train}$ are reflected into the generated electron microscope images $P_{m,k}^{gen}$. Based on the extracted features $f_{m,k,L^{train}}^{in}$, we obtain the generated electron microscope images $P_{m,k}^{gen}$ corresponding to the compound-property vector $c_{m,k}^{train}$ as follows:

$$P_{m,k}^{gen} = \mathcal{G}_{L^{gen}}(f_{m,k,L^{gen}}^{in}). \tag{3}$$

With the generation process, the encoder module $\mathcal{F}(\cdot)$ and generator module $\mathcal{G}_l(\cdot)$ are adversely trained with the discriminator module $\mathcal{D}(\cdot)$. These models are trained based on the loss functions provided by [27] as follows:

$$\min_{\mathcal{F}, \mathcal{G}} \max_{\mathcal{D}} \quad \mathbb{E}_{P_{m,k}^{real} \sim p_{real}}[\mathcal{D}(P_{m,k}^{real})] - \mathbb{E}_{P_{m,k}^{gen} \sim p_{gen}}[\mathcal{D}(P_{m,k}^{gen})]$$
$$+ \lambda \mathbb{E}_{P_{m,k} \sim p_{real}}[(\|\nabla_{P_{m,k}} \mathcal{D}(P_{m,k}^{real})\|_2 - 1)^2], \tag{4}$$

TABLE 1. $\text{FID}_{q,u}$ obtained by the proposed method.

	$u = 1$	$u = 2$	$u = 3$	$u = 4$	$u = 5$
$q = 1$	**132.86**	164.93	177.77	175.50	198.98
$q = 2$	159.33	**121.11**	181.02	188.33	201.11
$q = 3$	172.42	179.55	**130.10**	195.55	222.24
$q = 4$	192.33	188.88	195.44	**141.53**	249.31
$q = 5$	185.09	180.44	185.09	190.01	**135.01**

where λ and p_{gen} represent the regularization coefficient and probability distribution, followed by $P_{m,k}^{gen}$, respectively. With the above training, the encoder module $\mathcal{F}(\cdot)$ and generator module $\mathcal{G}_l(\cdot)$ can accurately generate images corresponding to the input compound-property.

B. COMPOUND-PROPERTY IMAGE RETRIEVAL

In this subsection, we introduce the compound-property retrieval procedure using the trained encoder module $\hat{\mathcal{F}}(\cdot)$ and the trained generator module $\hat{\mathcal{G}}_l(\cdot)$. Using electron microscope images, we can treat the compound-property retrieval as the image retrieval task. First, we generate an electron microscope image P^{query} from a query compound-property c^{query} using $\hat{\mathcal{F}}(\cdot)$ and $\hat{\mathcal{G}}_l(\cdot)$ as follows:

$$P^{query} = \hat{\mathcal{G}}_{L^{gen}}(f_{L^{gen}}^{qin}), \tag{5}$$

$$f_{l+1}^{qin} = f_l^{qs} \circ \frac{f_l^{qout} - \mu(f_l^{qout})}{\sigma(f_l^{qout})} + f_l^{qb}, \tag{6}$$

$$f_l^{qout} = \hat{\mathcal{G}}_l(f_l^{qin}), \tag{7}$$

$$f_l^{qs}, f_l^{qb} = \mathcal{A}_l(f^{qenc}), \tag{8}$$

$$f^{qenc} = \hat{\mathcal{F}}(z, c^{query}), \tag{9}$$

After that, we calculate the visual features from $f^{vis} \in \mathbb{R}^{D^{vis}}$ and $f_n^{vis} \in \mathbb{R}^{D^{vis}}$ from the generated electron microscope image P^{query} and electron microscope images P_n^{cand} of candidate compound-property c_n via the trained feature extractor $\mathcal{E}(\cdot)$ as follows:

$$f^{vis} = \mathcal{E}(P^{query}), \tag{10}$$

$$f_n^{vis} = \mathcal{E}(P_n^{cand}), \tag{11}$$

where D^{vis} represents the dimension of the extracted visual features. Then, the extracted features f^{vis} and f_n^{vis} are used to calculate similarities s_n as follows:

$$s_n = \frac{f^{vis} \cdot f_n^{vis}}{|f^{vis}||f_n^{vis}|}. \tag{12}$$

The proposed method calculates retrieval result indexes r_k by ranking the candidate images P_n^{cand} in descending order of s_n, where r_k indicates the index of k-th rank image obtained by the calculated ranking (*e.g.*, $P_{r_1}^{cand}$ represents the 1st rank image). Finally, visual and comprehensive machine learning-based support for the material discovery is realized by providing the retrieval results c_{r_k} with the corresponding electron microscope images $P_{r_k}^{cand}$.

TABLE 2. FID$_{q,u}$ ($q = u$) obtained by the proposed method and the comparative method.

	FID$_{1,1}$	FID$_{2,2}$	FID$_{3,3}$	FID$_{4,4}$	FID$_{5,5}$	mean
ACGAN	154.28	145.29	167.33	156.04	163.01	157.19
PM	**132.86**	**121.11**	**130.10**	**141.53**	**135.01**	**132.12**

TABLE 3. MAP@k obtained by the proposed method and the comparative method.

	MAP@5	MAP@10	MAP@15	MAP@20
Random	0.128	0.120	0.142	0.152
ACGAN	0.204	0.243	0.276	0.302
PM	**0.274**	**0.326**	**0.347**	**0.360**

IV. EXPERIMENTAL RESULTS AND DISCUSSIONS

A. EXPERIMENTAL SETTINGS

To evaluate the effectiveness of the proposed method, we collected the dataset with compound-property-electron microscope image pairs. The collected dataset consists of 156 electron microscope images and corresponding compound-property. Each electron microscope image is in grayscale with a resolution of $1{,}536 \times 1{.}024$ pixels. In our experiments, we randomly divided 156 electron microscope images into 151 $(= M)$ and 5 images for training and test, respectively. We conducted the experiments ten times. The average of each experiment result is shown in each table of experimental results. Additionally, each electron microscope image is divided into 256×256 resolution with 50 pixels slide width. After the patch division, 62,816 and 2,080 $(= N)$ patch images can be obtained for training and test images. However, to the best of our knowledge, we first attempt the compound-property retrieval, and it is difficult to use the other computer-aided material analysis methods as comparative methods.

We focused on evaluating the image generation capabilities and whether the relevant compound-property can be retrieved. Specifically, our method based on the auxiliary classifier GAN [22] (ACGAN) and a method that randomly ranks the candidate compound-property (Random) are used as the comparative methods. In our method, the visual feature extractor $\mathcal{E}(\cdot)$ is constructed following DenseNet121 model [30] trained on ImageNet [31].

B. QUANTITATIVE EXPERIMENTAL RESULTS

In this subsection, we quantitatively evaluate the effectiveness of the proposed method. The most important evaluation topic in our method is whether the generated images with certain compound-property are similar to the corresponding real images. Then, we evaluated our method using the popular evaluation metrics in image generation: Fréchet inception distance(FID) [32]. First, we extracted visual features from the real and generated images corresponding to the q-th $(q = 1, \ldots, Q;$ Q is the number of test compound-property) test compound-property through the DenseNet121 model

trained on ImageNet. Then, we calculated the mean μ_q^{real} (respectively, μ_q^{gen}) and covariance Σ_q^{real} (respectively, Σ_q^{gen}) from the features extracted from real (respectively, generated) images corresponding to the q-th test compound-property. Finally, we calculated FID$_{q,u}$ ($u = 1, \ldots, Q$) as follows:

$$\text{FID}_{q,u} = \mu + \Sigma, \tag{13}$$

$$\mu = |\mu_q^{\text{real}} - \mu_u^{\text{gen}}|^2, \tag{14}$$

$$\Sigma = \text{tr}(\Sigma_q^{\text{real}} + \Sigma_u^{\text{gen}} - 2\Sigma_q^{\text{real}}\Sigma_u^{\text{gen}}). \tag{15}$$

Moreover, FID$_{q,u}$ reveals the distance between the real images with q-th test compound-property and the generated images with u-th test compound-property. Following other information retrieval studies, we used the mean average precision@k (MAP@k) as follows:

$$\text{MAP@}k = \frac{1}{Q} \sum_q \text{AP}_{q,k}, \tag{16}$$

$$\text{AP}_{q,k} = \sum_{i=1}^{k} \frac{\text{Pr}_{q,i}}{k}, \tag{17}$$

$$\text{Pr}_{q,k} = \frac{g_{q,k}}{k}, \tag{18}$$

where $g_{q,k}$ represents the number of accurately retrieved relevant compound-property in the top-k retrieval results using the q-th test compound-property as a query. Here, we define compound-property similar to the query as relevant compound-property.

The experimental results are shown in Tables 1, 2, and 3. As presented in Table 1, the values of $q = u$ are lower than the values of $q \neq u$. This means that the proposed method generates images that are more similar to the images with the corresponding compound-property than the images with a non-corresponding compound-property. Table 2 shows that the proposed method outperforms ACGAN. These results show that our image generation model can generate images corresponding to the input compound-property than a method based on the ACGAN. Furthermore, Table 3 shows that our method can retrieve the corresponding compound-property more accurately than the other methods. These results confirm the effectiveness of the proposed method.

C. QUALITATIVE EXPERIMENTAL RESULTS

In this subsection, we evaluate the effectiveness of the proposed method through qualitative experiments. In the qualitative experiments, we asked material technologists to evaluate the generated images. First, we collected the generated and real images corresponding to the test compound-property. Then, we simultaneously showed the generated and real

TABLE 4. Percentage of technologists who misidentified the generated image as the real image.

	Sample 1	Sample 2	Sample 3	Sample 4	Sample 5	Sample 6	Sample 7	Mean
ACGAN	0.30	0.20	0.20	0.20	0.30	0.30	0.30	0.27
PM	**0.50**	**0.50**	**0.40**	**0.50**	**0.40**	**0.50**	**0.40**	**0.46**
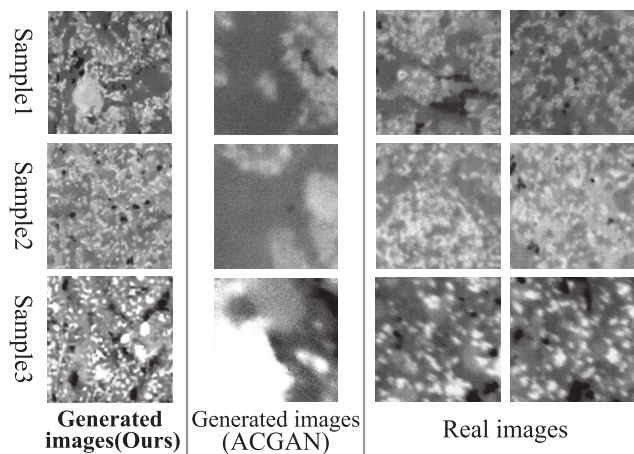
FIGURE 4. Real electron microscope images of rubber materials, generated images using the proposed method, and generated images using the comparative method.

images to the technologist and asked them to identify the real image from them. In the experiments, ten technologists evaluated the same seven generated and real images. Finally, we calculated the percentage of technologists who misidentified the generated image as the real image.

The experimental results and samples are shown in Table 4 and Fig. 4. Table 4 shows the percentage of technologists who misidentified the generated image as the real image. As presented in Table 4, technologists misidentify the images generated using the proposed method compared with the comparative method. These results show that our image generation model can generate images similar to the real images than a method based on the ACGAN. Additionally, considering that the technologists usually see the electron microscope images and are asked to identify the real images, it is considered that the range of value in Table 4 is 0 to about 0.5. Thus, we consider that the mean value of the proposed method is comparatively higher, indicating that the proposed method can generate realistic electron microscope images. These results show that the generated images using the proposed method can be useful for visualizing the relationships between compound-property. Although we focus on the material compound-property retrieval in this paper, our method using the conditional image generation model may contribute to various retrieval tasks. In future studies, we will further examine these applications.

V. CONCLUSION

In this paper, we first tackle compound-property retrieval using electron microscope images for rubber material development. The proposed method realizes the compound-property retrieval using electron microscope image space by generating the images corresponding to the query compound-property. It enables material technologists to visually and comprehensively understand the relationships between materials. The experimental results show the effectiveness of the proposed method.

REFERENCES

[1] W. Mars and A. Fatemi, "A literature survey on fatigue analysis approaches for rubber," *Int. J. Fatigue*, vol. 24, no. 9, pp. 949–961, Sep. 2002.

[2] W. V. Mars and A. Fatemi, "Factors that affect the fatigue life of rubber: A literature survey," *Rubber Chem. Technol.*, vol. 77, no. 3, pp. 391–412, Jul. 2004.

[3] L. Shen and Q. Qian, "A virtual sample generation algorithm supporting machine learning with a small-sample dataset: A case study for rubber materials," *Comput. Mater. Sci.*, vol. 211, Aug. 2022, Art. no. 111475.

[4] B. Medasani, A. Gamst, H. Ding, W. Chen, K. A. Persson, M. Asta, A. Canning, and M. Haranczyk, "Predicting defect behavior in B2 intermetallics by merging ab initio modeling and machine learning," *npj Comput. Mater.*, vol. 2, no. 1, pp. 1–10, Dec. 2016.

[5] M. D. Jong, W. Chen, R. Notestine, K. Persson, G. Ceder, A. Jain, M. Asta, and A. Gamst, "A statistical learning framework for materials science: Application to elastic moduli of K-nary inorganic polycrystalline compounds," *Sci. Rep.*, vol. 6, no. 1, p. 34256, Oct. 2016.

[6] F. Legrain, J. Carrete, A. van Roekeghem, S. Curtarolo, and N. Mingo, "How chemical composition alone can predict vibrational free energies and entropies of solids," *Chem. Mater.*, vol. 29, no. 15, pp. 6220–6227, Aug. 2017.

[7] T. Kojima, T. Washio, S. Hara, and M. Koishi, "Search strategy for rare microstructure to optimize material properties of filled rubber using machine learning based simulation," *Comput. Mater. Sci.*, vol. 204, Mar. 2022, Art. no. 111207.

[8] R. Togo, N. Saito, K. Maeda, T. Ogawa, and M. Haseyama, "Rubber material property prediction using electron microscope images of internal structures taken under multiple conditions," *Sensors*, vol. 21, no. 6, p. 2088, Mar. 2021.

[9] Ł. Zedler, X. Colom, J. Cañavate, M. Saeb, J. T. Haponiuk, and K. Formela, "Investigating the impact of curing system on structure-property relationship of natural rubber modified with brewery by-product and ground tire rubber," *Polymers*, vol. 12, no. 3, p. 545, Mar. 2020.

[10] G. Haddad, R. K. Gupta, and K. L. Wong, "Visualization of multi-factor changes in HTV silicone rubber in response to environmental exposures," *IEEE Trans. Dielectr. Electr. Insul.*, vol. 21, no. 5, pp. 2190–2198, Oct. 2014.

[11] L. Ward, A. Dunn, A. Faghaninia, N. E. R. Zimmermann, S. Bajaj, Q. Wang, J. Montoya, J. Chen, K. Bystrom, M. Dylla, K. Chard, M. Asta, K. A. Persson, G. J. Snyder, I. Foster, and A. Jain, "Matminer: An open source toolkit for materials data mining," *Comput. Mater. Sci.*, vol. 152, pp. 60–69, Sep. 2018.

[12] O. Hoeber, "Information visualization for interactive information retrieval," in *Proc. Conf. Human Inf. Interact. Retr. (CHIIR)*, 2018, pp. 371–374.

[13] J. Guo, Y. Fan, L. Pang, L. Yang, Q. Ai, H. Zamani, C. Wu, W. B. Croft, and X. Cheng, "A deep look into neural ranking models for information retrieval," *Inf. Process. Manage.*, vol. 57, no. 6, Nov. 2020, Art. no. 102067.

[14] K. D. Onal, Y. Zhang, I. S. Altingovde, M. M. Rahman, P. Karagoz, A. Braylan, B. Dang, H.-L. Chang, H. Kim, Q. McNamara, A. Angert, E. Banner, V. Khetan, T. McDonnell, A. T. Nguyen, D. Xu, B. C. Wallace, M. D. Rijke, and M. Lease, "Neural information retrieval: At the end of the early years," *Inf. Retr. J.*, vol. 21, nos. 2–3, pp. 111–182, Jun. 2018.

[15] B. Mitra and N. Craswell, "Neural text embeddings for information retrieval," in *Proc. 10th ACM Int. Conf. Web Search Data Mining*, Feb. 2017, pp. 813–814.

[16] A. J. Bowles, G. D. Fowler, C. O'Sullivan, and K. Parker, "Sustainable rubber recycling from waste tyres by waterjet: A novel mechanistic and practical analysis," *Sustain. Mater. Technol.*, vol. 25, Sep. 2020, Art. no. e00173.

[17] M. Fumagalli, J. Berriot, B. D. Gaudemaris, A. Veyland, J.-L. Putaux, S. Molina-Boisseau, and L. Heux, "Rubber materials from elastomers and nanocellulose powders: Filler dispersion and mechanical reinforcement," *Soft Matter*, vol. 14, no. 14, pp. 2638–2648, 2018.

[18] K. Bisht and P. V. Ramana, "Waste to resource conversion of crumb rubber for production of sulphuric acid resistant concrete," *Construct. Building Mater.*, vol. 194, pp. 276–286, Jan. 2019.

[19] Z. Pan, W. Yu, X. Yi, A. Khan, F. Yuan, and Y. Zheng, "Recent progress on generative adversarial networks (GANs): A survey," *IEEE Access*, vol. 7, pp. 36322–36333, 2019.

[20] X. Yan, J. Yang, K. Sohn, and H. Lee, "Attribute2Image: Conditional image generation from visual attributes," in *Proc. Eur. Conf. Comput. Vis.* Cham, Switzerland: Springer, 2016, pp. 776–791.

[21] C. Oeldorf and G. Spanakis, "LoGANv2: Conditional style-based logo generation with generative adversarial networks," in *Proc. 18th IEEE Int. Conf. Mach. Learn. Appl. (ICMLA)*, Dec. 2019, pp. 462–468.

[22] A. Odena, C. Olah, and J. Shlens, "Conditional image synthesis with auxiliary classifier GANs," in *Proc. Int. Conf. Mach. Learn.*, 2017, pp. 2642–2651.

[23] D. P. Kingma and M. Welling, "Auto-encoding variational Bayes," 2013, *arXiv:1312.6114*.

[24] A. Creswell, T. White, V. Dumoulin, K. Arulkumaran, B. Sengupta, and A. A. Bharath, "Generative adversarial networks: An overview," *IEEE Signal Process. Mag.*, vol. 35, no. 1, pp. 53–65, Jan. 2018.

[25] J. Ho, X. Chen, A. Srinivas, Y. Duan, and P. Abbeel, "Flow++: Improving flow-based generative models with variational dequantization and architecture design," in *Proc. Int. Conf. Mach. Learn. (PMLR)*, 2019, pp. 2722–2730.

[26] M. Arjovsky, S. Chintala, and L. Bottou, "Wasserstein generative adversarial networks," in *Proc. Int. Conf. Mach. Learn. (PMLR)*, 2017, pp. 214–223.

[27] I. Gulrajani, F. Ahmed, M. Arjovsky, V. Dumoulin, and A. C. Courville, "Improved training of Wasserstein GANs," in *Proc. Adv. Neural Inf. Process. Syst.*, vol. 30, 2017, pp. 1–11.

[28] T. Karras, T. Aila, S. Laine, and J. Lehtinen, "Progressive growing of GANs for improved quality, stability, and variation," 2017, *arXiv:1710.10196*.

[29] X. Huang and S. Belongie, "Arbitrary style transfer in real-time with adaptive instance normalization," in *Proc. IEEE Int. Conf. Comput. Vis. (ICCV)*, Oct. 2017, pp. 1510–1519.

[30] G. Huang, Z. Liu, L. Van Der Maaten, and K. Q. Weinberger, "Densely connected convolutional networks," in *Proc. IEEE Conf. Comput. Vis. Pattern Recognit. (CVPR)*, Jul. 2017, pp. 2261–2269.

[31] J. Deng, W. Dong, R. Socher, L.-J. Li, K. Li, and L. Fei-Fei, "ImageNet: A large-scale hierarchical image database," in *Proc. IEEE Conf. Comput. Vis. Pattern Recognit.*, Jun. 2009, pp. 248–255.

[32] M. Heusel, H. Ramsauer, T. Unterthiner, B. Nessler, and S. Hochreiter, "GANs trained by a two time-scale update rule converge to a local Nash equilibrium," in *Proc. Adv. Neural Inf. Process. Syst.*, 2017, pp. 6626–6637.

RINTARO YANAGI (Graduate Student Member, IEEE) received the B.S. degree in electronics and information engineering from Hokkaido University, Japan, in 2019, and the M.S. degree from the Graduate School of Information Science and Technology, Hokkaido University, in 2021, where he is currently pursuing the Ph.D. degree. His research interest includes machine learning and its applications. He is a Student Member of ACM.

REN TOGO (Member, IEEE) received the B.S. degree in health sciences from Hokkaido University, Japan, in 2015, and the M.S. and Ph.D. degrees from the Graduate School of Information Science and Technology, Hokkaido University, in 2017 and 2019, respectively. He is a Radiological Technologist. He is currently a Specially Appointed Assistant Professor with the Laboratory of Media Dynamics, Faculty of Information Science and Technology, Hokkaido University. His research interest includes machine learning and its applications. He is a member of ACM and IEICE.

KEISUKE MAEDA (Member, IEEE) received the B.S., M.S., and Ph.D. degrees in electronics and information engineering from Hokkaido University, Japan, in 2015, 2017, and 2019, respectively. He is currently a Specially Appointed Assistant Professor with the Faculty of Information Science and Technology, Hokkaido University. His research interests include multi-modal signal processing and machine learning and its applications. He was a TPC Member of IEEE GCCE2019. He is a member of IEICE. He was the Organized Session Co-Chair of IEEE GCCE2020.

TAKAHIRO OGAWA (Senior Member, IEEE) received the B.S., M.S., and Ph.D. degrees in electronics and information engineering from Hokkaido University, Japan, in 2003, 2005, and 2007, respectively. He joined the Graduate School of Information Science and Technology, Hokkaido University, in 2008, where he is currently an Associate Professor with the Faculty of Information Science and Technology. His research interests include AI, the IoT, and big data analysis for multimedia signal processing and its applications. He is a member of ACM, IEICE, and ITE. He was the Special Session Chair of IEEE ISCE2009, the Doctoral Symposium Chair of ACM ICMR2018, the Organized Session Chair of IEEE GCCE2017-2020, the TPC Vice Chair of IEEE GCCE2018, and the Conference Chair of IEEE GCCE2019. He has been an Associate Editor of *ITE Transactions on Media Technology and Applications*.

MIKI HASEYAMA (Senior Member, IEEE) received the B.S., M.S., and Ph.D. degrees in electronics from Hokkaido University, Japan, in 1986, 1988, and 1993, respectively. She joined the Graduate School of Information Science and Technology, Hokkaido University, as an Associate Professor, in 1994. She was a Visiting Associate Professor with Washington University, St. Louis, MO, USA, from 1995 to 1996. She is currently a Professor with the Faculty of Information Science and Technology, Hokkaido University. She is the Director of the International Coordination and Publicity, Institute of Electronics, Information and Communication Engineers (IEICE). Her research interests include image and video processing and its development into semantic analysis. She is a fellow of ITE and a member of IEICE and ASJ. She has been the Vice-President of the Institute of Image Information and Television Engineers, Japan (ITE), and an Editor-in-Chief of *ITE Transactions on Media Technology and Applications*.

• • •